$K\alpha$ transition probabilities for fluorinelike ions from neon to gold: *Ab initio* relativistic coupled-cluster calculations

Chiranjib Sur, Sultana N. Nahar, and Anil K. Pradhan
Department of Astronomy, The Ohio State University, Columbus, Ohio, 43210 USA
(Received 7 January 2008; revised manuscript received 7 March 2008; published 15 May 2008)

We have applied the relativistic Fock-space coupled-cluster theory to calculate $K\alpha$ transition properties of F-like ions for a number of elements throughout the periodic table. A state-specific form of the coupled-cluster method for electron detachment has been used to calculate the $K\alpha$ energies and line strengths. The computed energies are used to determine the transition probabilities for more than 30 elements to study the Z dependencies for $Z=10-79$. This application of a variant of coupled-cluster theories to study the $K\alpha$ transitions should be the most accurate determination of these transition probabilities to date. The most important finding in this paper is the crossover of $K\alpha_1$ and $K\alpha_2$ at high Z. In general, for lighter ions, $K\alpha_2$ is higher in magnitude than $K\alpha_1$, but at $Z=41-42$ they are switched. In addition, the results demonstrate the variation with Z of the $K\alpha_2$ A values along the Periodic Table. The astrophysical significance in the analysis of $K\alpha$ lines, important in x-ray astronomy, is pointed out.

DOI: 10.1103/PhysRevA.77.052502 PACS number(s): 31.15.bw, 31.15.A−, 31.15.V−, 32.70.Cs

I. INTRODUCTION

Many aspects of $K\alpha$ transitions in atoms and ions are of considerable interest. To understand the physics behind the interaction of electromagnetic radiation, particularly x rays, with hollow atoms and ions, ionized nanoparticles, and atomic clusters, knowledge of $K\alpha$ transition probabilities is essential. Their importance in x-ray astronomy is well known, for both light elements such as oxygen [1] and heavy elements such as iron [2], from the observations made with Chandra, XMM-Newton, and other x-ray space observatories. However, the study of $K\alpha$ lines goes back much farther to many experimental and theoretical studies, and to the derivation of semiempirical laws such as Moseley's law. Possibly the most recent interest in x-ray–K-shell interactions with heavy elements is in biophysics. Experiments have shown that x-ray irradiation of gold nanoparticles embedded in cancerous tumors may be effective in their treatment [3,4]. Further studies are needed in order to model the myriad Auger processes, including $K\alpha$ transitions, triggered by K-shell ionization and excitation.

From a theoretical point of view, the atomic physics of heavy elements poses considerable challenge owing to both the relativistic and electron correlation effects that must be treated together in an accurate manner. The calculation of $K\alpha$ transitions is not trivial because of the presence of multielectron inner-shell vacancies. To our knowledge, this is the first time relativistic coupled-cluster (RCC) theory, one of the most accurate many-body theories for atoms and ions, has been applied to study this problem. Recently, we have studied the resonant enhancement of K-edge x-ray absorption by gold nanoparticles which have potential applications in biomedicine [5]. This work supplements our finding of the K-edge fluorescence yield for high-Z elements [5,6]. Several groups have studied the production of $K\alpha$ radiation due to high-intensity lasers for light and heavy elements [7–9]. The present study of $K\alpha$ transitions also enables us to explore the physics of "hollow atoms" which are also of contemporary interest [10–12]. In this paper, we calculate the $K\alpha$ transitions for a number of elements throughout the Periodic Table using RCC theory, which is equivalent to all-order many-body perturbation theory and size extensive in nature.

All ions from H-like to F-like electronic configurations give rise to $K\alpha$ transition arrays belonging to the $1s \rightarrow 2p$ complexes. In this paper, we study the $K\alpha_1$ and $K\alpha_2$ transitions in F-like ions, with a vacancy in the K or the L shell,

$$1s2s^22p^6(^2S_{1/2}) \rightarrow 1s^22s^22p^5(^2P^0_{3/2,1/2}). \tag{1}$$

In general, the second transition ($K\alpha_2$) is larger in magnitude for lighter elements, but we have found a crossover Z where the first transition ($K\alpha_1$) become larger in magnitude as compared to the second one ($K\alpha_2$). The calculations span most of the periodic table, enabling us to also examine the relative Z dependency, which may be of practical value in astrophysical and technological applications.

The structure of the paper is as follows. The following section (Sec. II) gives a brief description of the RCC theory for electron detachment processes, which can be found in more detail in Ref. [14]. The theory for the state-specific transitions using RCC calculations and computational details have also been outlined there. In Sec. III we give the tabular description of transition probabilities for a number of F-like ions throughout the periodic table and discuss the results. Finally, in Sec. IV, we highlight our findings and draw the conclusions.

II. THEORETICAL AND COMPUTATIONAL DETAILS

Relativistic coupled-cluster theory is based on the no-virtual-pair approximation along with appropriate modification of orbital form and potential terms [13]. One begins with the Dirac-Coulomb Hamiltonian (H) for an N-electron atom, which is expressed as

$$H = \sum_{i=1}^{N} [c\vec{\alpha}_i \cdot \vec{p}_i + \beta mc^2 + V_{\text{nuc}}(r_i)] + \sum_{i<j}^{N} \frac{e^2}{r_{ij}}, \tag{2}$$

with all the standard notations often used. The normal ordered form of the above Hamiltonian is given by

$$\mathcal{H} = H - \langle\Phi|H|\Phi\rangle$$
$$= H - E_{\mathrm{DF}}$$
$$= \sum_{ij} \langle i|\mathrm{f}|j\rangle\{a_i^\dagger a_j\} + \frac{1}{4}\sum_{i,j,k,l} \langle ij||kl\rangle\{a_i^\dagger a_j^\dagger a_l a_k\}, \quad (3)$$

where

$$\langle ij||kl\rangle = \langle ij|\frac{1}{r_{12}}|kl\rangle - \langle ij|\frac{1}{r_{12}}|lk\rangle. \quad (4)$$

Here f and E_{DF} are the one-electron Fock operator and the Dirac-Fock energy, respectively, and $|\Phi\rangle$ is the N-electron Dirac-Fock reference state. a_i ($a_i^\dagger$) is the annihilation (creation) operator for the ith electron and $\{\cdots\}$ denotes the normal ordering of the creation and annihilation operators with respect to the common vacuum $|\Phi\rangle$. The N-electron atom is then correlated using the *valence universal* wave operator (Ω) which has two parts; one corresponds to the closed-shell part and the other to the valence part. The correlation operator (wave operator) is expressed as

$$\Omega = \exp(T)\{\exp(S)\}. \quad (5)$$

The part $\exp(T)$ corresponds to the closed-shell correlation operator and in the single- and double-(SD) excitation approximation it takes the form

$$T = \sum_{a,p} \{a_p^\dagger a_a\} t_a^p + \frac{1}{4}\sum_{a,b,p,q} \{a_p^\dagger a_q^\dagger a_b a_a\} t_{ab}^{pq}. \quad (6)$$

To solve the coupled-cluster amplitude for the closed shell we define the effective Hamiltonian as $H_{\mathrm{eff}} = \exp(-T)H\exp(T)$. This effective Hamiltonian is not Hermitian in nature and therefore the energy E is not an upper bound of the ground state energy. Once the excitation amplitudes are known for the core sector (closed shell) using the CCSD approximation, the atom is then correlated by the ionization operator for the valence $(1h,0p)$ sector. Using the Fock-space partitioning scheme [14] one electron is then ionized from the core as

$$\mathrm{atom}(0,0) - e \rightarrow \mathrm{ion}(1,0). \quad (7)$$

When the valence electron is detached from the occupied orbital of the ion in the core sector we get the ion for the $(1h,0p)$ sector. The corresponding cluster operator is denoted by S which follows from Eq. (5). In the single- and double-excitation approximation S is expressed as

$$S = \sum_{a\neq b} \{a_a^\dagger a_b\} s_b^a + \sum_{c,b,p} \{a_p^\dagger a_a^\dagger a_b a_c\} s_{bc}^{ap}. \quad (8)$$

These cluster operators are then used to construct the effective Hamiltonian, which in turn gives the state energies and the cluster amplitudes upon diagonalization. The methodology have been explained in detail in Ref. [14]. We have also studied the effect of higher-order excitations (triples, quadruples, etc.) and deexcitations by using a unitary approach known as unitary coupled-cluster theory. The higher-order amplitudes do not affect the result in the significant digits for F-like ions. More details about the effect of higher-order excitations for atomic coupled-cluster calculations can be found in Ref. [15].

In this paper we are interested in computing the electric dipole transition matrix elements $K\alpha_1(1s^22s^22p^6\ ^2S_{1/2} \rightarrow 1s^22s^22p^5\ ^2P_{3/2})$ and $K\alpha_2(1s^22s^22p^6\ ^2S_{1/2} \rightarrow 1s^22s^22p^5\ ^2P_{1/2})$, respectively. We use the RCC theory to determine the $^2S_{1/2}$ and $^2P_{1/2,3/2}$ states separately and the RCC calculation is therefore considered as specific for each state. The general transition matrix element for a transition from an initial state (i) to a final state (f) is defined as

$$M_{fi} = \langle\Psi_f|O^{(k)}|\Psi_i\rangle, \quad (9)$$

where $|\Psi_f\rangle = 1s^22s^22p^5\ ^2P_{1/2,3/2}$ and $|\Psi_i\rangle = 1s2s^22p^6\ ^2S_{1/2}$ are the final and initial many-body states. In spectroscopic (x-ray) notation, the initial state is labeled as K and the final states are L_2 and L_3, respectively.

The one-electron orbitals are generated by solving the Dirac-Fock equations using the technique of finite basis set expansion [16] of a large even-tempered basis set $(35s,32p,25d,25f)$ of Gaussian-type orbitals for all the ions, using the form

$$F_{i,k}(r) = r^k \exp(-\alpha_i r^2) \quad (10)$$

with $k=0,1,2,\ldots$ for $s,p,d,\ldots$ type functions, respectively. The exponents are determined by the even-tempering condition

$$\alpha_i = \alpha_0 \beta^{i-1}. \quad (11)$$

The small components are obtained by imposing the kinetic balance condition to avoid continuum dissolution. More details can be found in [16]. We have assumed that the nucleus has a Fermi-type finite structure [17] with the form

$$\rho = \frac{\rho_0}{1+\exp[(r-c/a)]}, \quad (12)$$

where the parameter c is the half charge radius and a is related to skin thickness, defined as the interval of the nuclear thickness in which the nuclear charge density falls from near one to near zero. Excitations (single and double, namely, SD) from all the core orbitals have been considered and we have checked the convergence of the size of the active space for the actual RCC calculations. Convergence of the results has been checked to eliminate uncertainties arising from the basis set. We have studied carefully the effects of higher-angular-momentum states in two steps, first by excluding the f states throughout and second by including g states. We have studied the computed energy values and the transition matrix elements up to four significant figures to ensure that error arising from the chosen basis set is minimized. The exponents are chosen by carefully studying the normalization and overlap integrals of the single-particle orbitals.

III. RESULTS AND DISCUSSIONS

Here we present the energy differences in eV and the transition probabilities for the two transitions mentioned above. Table I contains the difference energies (in eV) and

TABLE I. Transition probabilities (in s^{-1}) for F-like ions. The terminology $x(y)$ means $x \times 10^y$.

Ion	Atomic number (Z)	$K\alpha_2$		$K\alpha_1$	
		ΔE (eV)	A (s^{-1})	ΔE (eV)	A (s^{-1})
Ne II	10	843.14	2.234(12)	843.57	1.674(12)
Mg IV	12	1251.43	4.002(12)	1252.09	3.238(12)
Al V	13	1486.53	6.337(12)	1487.37	3.423(12)
Si VI	14	1741.47	1.081(13)	1742.54	0.497(13)
P VII	15	2018.24	1.605(13)	2019.59	0.549(13)
S VIII	16	2314.53	1.810(13)	2316.25	0.666(13)
Cl IX	17	2631.67	2.623(13)	2633.84	0.741(13)
Ar X	18	2969.73	3.405(13)	2972.47	0.792(13)
K XI	19	3328.64	4.257(13)	3332.07	0.852(13)
Sc XIII	21	4110.22	8.744(13)	4115.48	0.947(13)
Ti XIV	22	4532.18	1.012(14)	4538.62	0.118(14)
V XV	23	4975.37	1.175(14)	4983.19	0.132(14)
Cr XVI	24	5439.71	1.385(14)	5449.14	0.194(14)
Mn XVII	25	5925.62	1.777(14)	5936.91	0.259(14)
Fe XVIII	26	6432.86	1.842(14)	6446.30	0.414(14)
Co XIX	27	6961.33	2.378(14)	6977.21	0.529(14)
Ni XX	28	7511.41	2.678(14)	7530.06	0.632(14)
Cu XXI	29	8083.14	2.988(14)	8104.92	0.842(14)
Zn XXII	30	8676.58	3.467(14)	8701.87	1.09(14)
Ga XXIII	31	9291.76	4.079(14)	9321.00	1.320(14)
Ge XXIV	32	9927.94	4.662(14)	9961.59	1.727(14)
As XXV	33	10589.76	5.552(14)	10628.31	1.882(14)
Se XXVI	34	11270.54	5.902(14)	11314.53	2.285(14)
Br XXVII	35	11974.07	6.578(14)	12024.07	2.648(14)
Nb XXXIII	41	16670.42	1.364(15)	16770.97	1.325(15)
Mo XXXIV	42	17532.85	1.506(15)	17644.67	1.533(15)
Tc XXXV	43	18419.02	1.670(15)	18543.06	1.694(15)
Rh XXXVII	45	20262.25	1.985(15)	20413.80	2.031(15)
Ag XXXIX	47	22200.98	2.412(15)	22384.55	2.456(15)
Cd XL	48	23206.55	2.647(15)	23408.00	2.707(15)
In XLI	49	24236.50	2.887(15)	24457.15	3.021(15)
Sn XLII	50	25290.91	3.111(15)	25532.18	3.268(15)
Sb XLIII	51	26369.45	3.405(15)	26632.81	3.781(15)
Xe XLVI	54	29760.80	4.475(15)	29760.80	4.505(15)
La XLIX	57	33380.77	5.656(15)	33812.33	5.846(15)
Nd LII	60	37238.86	7.054(15)	37781.52	7.198(15)
Sm LIV	62	39946.51	7.679(15)	40575.09	8.352(15)
Au LXXI	79	67764.90	2.158(16)	69667.54	2.312(16)

transition probabilities (in s^{-1}) for $K\alpha_2$ and $K\alpha_1$ transitions for F-like ions from Ne through K, Sc through Br, Nb through Rh, Ag, Cd through Sb, Xe, La, Nd, Sm, and Au. We have observed in general that the transition probabilities (A) for $K\alpha_2$ are greater than for $K\alpha_1$ but as we increase the atomic numbers we find a region of crossover. Particularly up to Z=41 (Nb), the A value for $K\alpha_2$ is greater than for $K\alpha_1$ but at Z=42 (Mo) we find a crossover, and for all the other high-Z elements (42 onward), the A value for $K\alpha_1$ is greater in magnitude than for $K\alpha_2$. These results are presented graphically in Figs. 1 and 2. In Fig. 1 we have divided the plot into two regions, namely, for $Z<30$ and $Z>30$. Figure 1(a) shows the variation of A values for $Z<30$ and Fig. 1(b) corresponds to the variation of A values for $Z>30$. Figure 2 is a scaled image for the Z dependencies from Z=35 to 57. In Figs. 1(b) and 2, have pointed out the region of crossover where the A values for $K\alpha_1$ become higher in magnitude as compared to those for $K\alpha_2$.

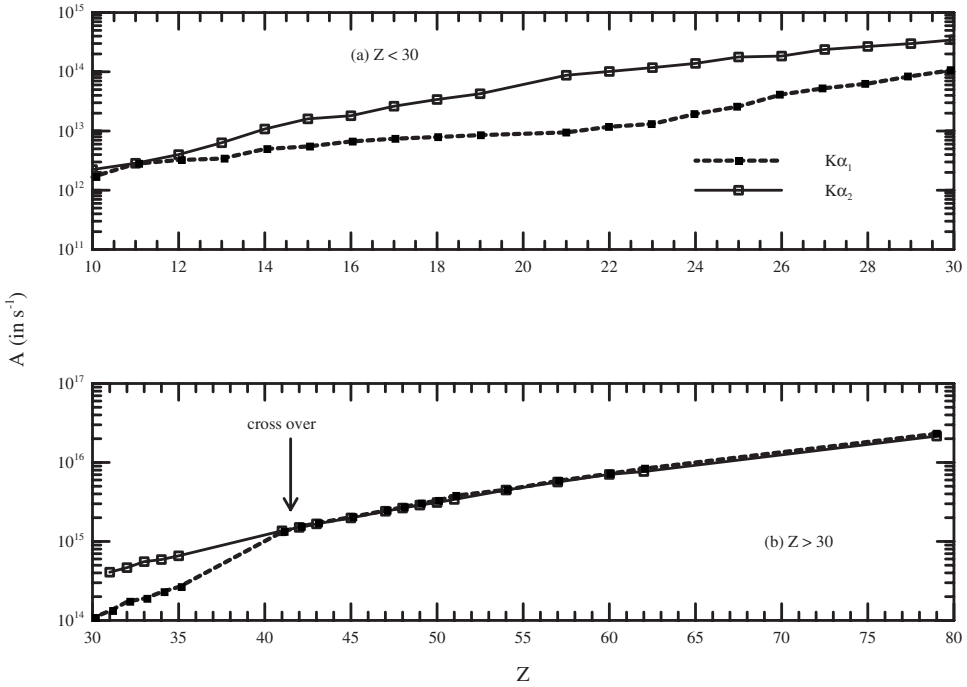

FIG. 1. Z dependencies of A values for (a) $Z<30$ and (b) $Z>30$.

In Table II we have compared our results with two those from well-known codes, GRASP [18] and SUPERSTRUCTURE [19]. The comparison of the fine structure (FS) splittings of the $2p^5\,{}^2P^o_{1/2,3/2}$ state with the experimental data yields a range of 3–6 % agreement for the available values. For example, the FS splittings for Fe XVIII, Zn XXII, and Ga XXIII are 13.4321 (12.7182), 25.2961 (24.4085), and 29.2409 (28.3180) eV, respectively, where the values given in parentheses are the experimentally observed values obtain from the NIST tables [20]. For Fe XVIII the zeroth-order (Dirac-Fock) value turns out to be 13.07 eV and this can be explained from the theoretical structure of the coupled-cluster equations. In SUPERSTRUCTURE, one-body and two-body terms (e.g. Breit interaction) of the Breit-Pauli Hamiltonian, are taken into account. The relative magnitude of the Breit interaction is α^2 times smaller than that of the Coulomb interaction, where α is the fine structure constant, and it is considered to be important for high-Z elements. For our case, all the ionic species considered are fluorinelike and only the nuclear charges are different for different ions. In addition to the Breit interaction, inclusion of QED effects [21] such as the self-energy and the vacuum polarization may be necessary for heavy atoms. We have not included Breit interaction and QED effects for determination of energy and line strengths. In the other two codes used here, GRASP is based on the Dirac-Fock formulation and does not employ the Breit interaction; QED effects are not considered in either SUPERSTRUCTURE or GRASP. The differences between the RCC values and the observed energies will give us a measure of the uncertainties for the determination of the energies of K, and $L_{2,3}$ states.

As mentioned, the $K\alpha$ lines are the most important spectral features in x-ray astronomy (e.g., [1]). Usually, these are due to electron impact excitation or electron-ion recombina-

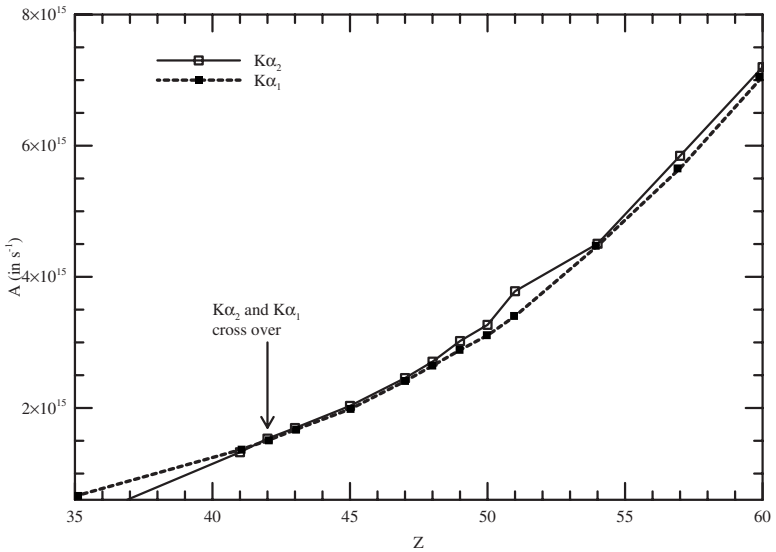

FIG. 2. Z dependencies of A values of F-like ions for the range Z=35–57, showing the crossover between $K\alpha_1$ and $K\alpha_2$ at Z=41–42.

TABLE II. Comparison of energies (in keV) and transition probabilities (in s^{-1}) for F-like Au with results from other codes. The terminology $x(y)$ means $x \times 10^{y}$.

	$K\alpha_2$		$K\alpha_1$	
Ions	ΔE (keV)	A (s^{-1})	ΔE (keV)	A (s^{-1})
RCC	67.765	2.158(16)	69.667	2.312(16)
SUPERSTRUCTURE [19]	67.383	1.59(16)	69.265	3.42(16)
GRASP2 [18]	67.871	1.93(16)	69.793	2.102(16)

tion of H-like and He-like ions ([22] and references therein). However, one of the most remarkable observations in astrophysics in recent years is the detection of $K\alpha$ lines from "neutral" iron from relatively "cold" plasma in accretion disks around black holes. The unresolved $K\alpha$ feature is gravitationally redshifted according to the general theory of relativity. All Fe ions with a filled $2p$ subshell and a vacancy in the $1s$ subshell would give rise to this feature with rest-frame energy at ~6.4 keV, where the line profile peaks but has a long and asymmetric redward component extending down to energies well below 6 keV [2]. In fact, the iron may *not* be in neutral ionization state at all, but in any ionization state from Fe I to Fe XVII. Table I gives the energies of the $K\alpha_1$ and $K\alpha_2$ transitions in Fe I to great precision. It is expected that all such lines in Fe I to Fe XVII will also be at about the same energy, since outer-shell correlations will be of little importance in affecting the inner $K\alpha$ transitions. Thus far the gravitational $K\alpha$ redshift has not been seen in any other element, but it should be possible in principle. The high accuracy of the transition energies and probabilities in Table I should also be applicable to modeling and calibration of these lines in laboratory sources.

IV. CONCLUSIONS

In conclusion, in this paper we have applied a variant of relativistic coupled-cluster theory to determine the ionization energies of the K shell, and $K\alpha$ transition probabilities. A number of ions in the fluorine isoelectronic sequence have been studied and the $K\alpha_{1,2}$ transition probabilities are analyzed; they are of much contemporary importance, e.g., in nanospectroscopy, applications to biomedicine, astronomy, hollow atoms and ions, etc. Whereas the overall behavior of the $K\alpha$ A values varies monotonically with Z, there are significant relative differences. In particular, we have observed the variance of the $K\alpha$ transitions with increasing atomic number and found a crossover region where the $K\alpha_1$ transition turns out be higher in magnitude compared to $K\alpha_2$. This work leads us to examine other isoelectronic sequences, which are under study.

ACKNOWLEDGMENTS

We thank Professor R. K. Chaudhuri for various discussions and help. The computational work was carried out at the Ohio Supercomputer Center in Columbus Ohio. This work was partially supported by a grant from NASA (SNN).

[1] A. K. Pradhan, G. X. Chen, F. Delahaye, and S. N. Nahar, Mon. Not. R. Astron. Soc. **341**, 1268 (2003).
[2] Y. Tanaka *et al.*, Nature (London) **375**, 659 (1996).
[3] J. F. Hainfield, D. N. Slatkin, and H. M. Smilowitz, Phys. Med. Biol. **49**, N309 (2004).
[4] S. H. Cho, Phys. Med. Biol. **50**, N163 (2005).
[5] A. K. Pradhan, S. N. Nahar, Y. Yu, C. Sur, M. Montenegro, M. Mrozik, and R. Pitzer (unpublished).
[6] S. N. Nahar, C. Sur, and A. K. Pradhan, J. Quant. Spectrosc. Radiat. Transf. doi: 10.1016/j.jqsrt.2008.01.010 (2008).
[7] U. Andiel, K. Eidmann, and K. Witte, Phys. Rev. E **63**, 026407 (2001).
[8] N. Zhavoronkov *et al.*, Appl. Phys. Lett. **86**, 244107 (2005).
[9] M. Berger and J. W. Motz, Nucl. Instrum. Methods Phys. Res. B **226**, 805 (1994).
[10] K. Moribayashi, A. Sasaki, and A. Zhidkov, Phys. Scr., T **92**, 185 (2001).
[11] H. Winter and F. Aumayr, J. Phys. B **32**, R39 (1999).
[12] F. Rosmej *et al.*, J. Quant. Spectrosc. Radiat. Transf. **65**, 477 (2000).
[13] E. Eliav, U. Kaldor, and Y. Ishikawa, Phys. Rev. A **50**, 1121 (1994).
[14] C. Sur and R. K. Chaudhuri, J. Phys. B **37**, 4127 (2004).
[15] C. Sur and R. K. Chaudhuri, Chem. Phys. Lett. **442**, 150 (2007).
[16] R. K. Chaudhuri, P. K. Panda, and B. P. Das, Phys. Rev. A **59**, 1187 (1999).
[17] O. Matsouka and S. Huzinaga, Chem. Phys. Lett. **140**, 567 (1987).
[18] K. G. Dyall, I. P. Grant, C. T. Johnson, F. A. Parpia, and E. P. Plummer, Comput. Phys. Commun. **55**, 424 (1989).
[19] W. Eissner, M. Jones, and H. Nussbaumer, Comput. Phys. Commun., **8**, 270 (1974).
[20] http://www.nist.gov/
[21] H. M. Quiney, I. P. Grant, and S. Wilson, J. Phys. B **20**, 1413 (1987).
[22] J. Oelgoetz, C. J. Fontes, H. L. Xhang, M. Montenegro, S. N. Nahar, and A. K. Pradhan, Mon. Not. R. Astron. Soc. **382**, 761 (2007).